# Long noncoding RNA RP11-704M14.1 acts as a sponge of miR-6756-5p to promote neuronal proliferation by regulating ALOX15 expression

Cao Ke[1,2], Gong Ru[1,2], Wang Jiancun[3], Yu Cong[4], Zhang Yisong[4], Zheng Ping[4]

[1]Brain Injury Centre, Department of Neurosurgery, Renji Hospital, Shanghai Jiao Tong University School of Medicine, Shanghai, China
[2]Shanghai Institute of Head Trauma, Shanghai, China
[3]Department of Neurosurgery, Third Affiliated Hospital of Naval Medical University, Shanghai, China
[4]Department of Neurosurgery, Shanghai Pudong New Area People's Hospital, Shanghai, China

**Corresponding author:**
Dr. Zheng Ping
Department of Neurosurgery
Shanghai Pudong New Area People's Hospital
Shanghai, China
E-mail: jojo_ras@126.com

**Submitted:** 11 March 2024; **Accepted:** 15 May 2024
**Online publication:** 12 June 2024

Arch Med Sci
DOI: https://doi.org/10.5114/aoms/188720


## Abstract

**Introduction:** Long noncoding RNAs (lncRNAs) mediate critical effects in central nervous system diseases; however, the exact role of lncRNAs in human traumatic brain injury (TBI) remains elusive. Considering the principles of primary prediction, targeted prevention, and personalized treatment medicine (PPPM), identifying specific novel biomarker associated with TBI and exploring the underlying mechanisms comprehensively are crucial steps towards achieving primary prediction, targeted prevention, and personalized treatment of TBI.
**Material and methods:** In this study, we integrated single-cell RNA sequencing (sc-RNA-seq) data and microarray chipset data for TBI to identify a competing endogenous RNA axis.
**Results:** We detected 11 clusters based on the sc-RNA-seq data and identified *Ifit1* as a marker gene co-expressed with ENST00000505646.1 (RP11-704M14.1). Additionally, the expression of *IFIT1* and RP11-704M14.1 was found to decrease with the severity of TBI. RP11-704M14.1 promoted neuronal proliferation, and its knockdown prevented this effect. Furthermore, we found that RP11-704M14.1 functions as a miR-6756-5p sponge and increases the expression of its target gene *ALOX15*.
**Conclusions:** Our results show that RP11-704M14.1 promotes neuronal proliferation by sponging miR-6756-5p and regulating *ALOX15* expression in brain insults; accordingly, targeting this lncRNA presents a promising avenue for advancing the transition from reactive medicine to PPPM in managing traumatic brain injury, potentially leading to significant clinical benefits.

**Key words:** competing endogenous RNA, long noncoding RNA, RP11-704M14.1, single-cell RNA sequencing, traumatic brain injury.

## Introduction

Traumatic brain injury (TBI) poses a significant public health challenge due to its association with neurodegeneration, cognitive deficits, and psychiatric disturbances [1, 2]. Although the precise molecular and pathological alterations following TBI remain poorly understood, noncoding RNAs, particularly long noncoding RNAs (lncRNAs), have emerged as pivotal players in disease

mechanisms and therapeutic target development [3]. A number of lncRNAs in the brain are specifically related to neuronal and synaptic function [4]. LncRNAs constitute a large class of post-transcriptional regulators, some of which can act as competing endogenous RNAs (ceRNAs) to inhibit microRNAs (miRNAs) in the brain [5, 6]. Notably, aberrant lncRNA expression has been documented in the hippocampi of rats subjected to TBI [7, 8]. Accumulating evidence has demonstrated that several lncRNA can inhibit the inflammatory response after TBI [9, 10].

ALOX15 is implicated in the inflammatory response of various diseases, including colitis, yet its role in TBI is not fully elucidated. Dysregulation of miRNAs has been observed in the context of post-TBI neuroinflammation, with specific miRNAs altering the inflammatory landscape [11–14]. We previously reported that reduced miR-195 expression facilitates neuronal proliferation to improve neurological outcome following TBI [15] and the lncRNA NKILA acts as a miR-195 sponge, leading to increased expression of the miR-195 target gene *NLRX1*, particularly in neocortical and hippocampal neurons [15]. Comprehensive analyses of lncRNAs in the brain may provide key insights into TBI; however, few studies have focused on ceRNAs in TBI and their diagnostic and therapeutic value [16].

In this study, we employed a data mining strategy, integrating single-cell RNA sequencing (sc-RNA-seq) and a bulk chipset data, to delineate and validate a ceRNA network implicated in TBI. We uncovered a novel ceRNA axis, RP11-704M14.1–miR-6756-5p–ALOX15, and explored its correlation with clinical manifestations using *in vitro* and *in vivo* brain injury models. This led us to hypothesize that RP11-704M14.1 may influence TBI pathogenesis through miR-6756-5p-mediated regulation of ALOX15.

## Material and methods

### Sample collection

For the sample collection, bioinformatical analysis, in-vitro and in-vivo study, we followed the methods of Dr. Zheng *et al.* 2022 [17]. Peripheral human blood samples were prospectively obtained and transferred into PAX RNA Tubes (BD, Shanghai, China) within one day after TBI [18]. Patients with TBI were recruited in 2019 based on initial head CT findings, which demonstrated brain contusions. The study protocol was approved by the local Ethics Committee in Shanghai Pudong New area People's Hospital (20170223-001 on March 7, 2017). The informed consent form was obtained as required. Patients with TBI were classified according to the GCS score as follows: severe group (GCS 3-8), moderate group (GCS 9-12) and mild group (GCS 13-15). Patients aged 18–65 years with a closed brain injury were included. The exclusion criteria were as follows: (1) severe complication with thoracic or abdominal injury, (2) serious previous diseases (such as thrombocytopenia and cancer), (3) refused blood collection.

### Data processing

The single-cell transcriptome dataset GSE160763 was downloaded from the Gene Expression Omnibus (GEO) database (http://www.ncbi.nlm.nih.gov/geo/) [19]. The chipset data from TBI patients were previously reported and used as an external verification here [18]. R (v. 4.0.2) was used for bioinformatical analysis.

### sc-RNA-seq analysis

The Seurat package was used for the sc-RNA seq study [20]. The dimensionality of data was reduced by principal component analysis (PCA) and t-distributed stochastic neighbor embedding (t-SNE). Marker genes for different clusters were identified using the Seurat package. All clusters were annotated using the SingleR package with a mouse dataset [21], and cell-cell communication was performed using the CellChat package [22]. Cluster biomarkers were identified using the Seurat package. Monocle 3.0 was used to for the pseudo-time analysis of clusters of interest [23].

### Identification and validation of cluster marker genes in the chipset data

The Agilent Human lncRNA Microarray 2019 (4*180k, Design ID:086188) was used to analyze 16 samples by OE Biotechnology Co., Ltd. (Shanghai, China).

### Construction of the prognostic model associated with necroptosis

Firstly, the genes related to necroptosis with prognostic value were preliminarily obtained by univariate COX analysis. Subsequently, prognostic necroptosis-related genes were further screened by the least absolute and selection operator (LASSO) regression, and the prognostic model was constructed. In this way, each cluster can be calculated with an necropotosis score (NCPS) through the formula. Based on the median value, patients in the cohort can be divided into high and low risk groups. We then explored the difference in prognosis between the two groups and assessed the accuracy of the model.

### Gene microarray

Total RNA was quantified by the NanoDrop ND-2000 (Thermo Scientific, San Francisco, CA, USA), and RNA integrity was assessed using the Agilent

Bioanalyzer 2100 (Agilent Technologies, Santa Clara, CA, USA) according to the manufacturer's protocols. In brief, total RNA was used for the synthesis of cDNA, which was used for cRNA synthesis and labeling with cyanine-3-CTP. The labeled cRNAs were hybridized onto the microarray chipset. After washing, the chipset was scanned using the Agilent Scanner G2505C (Agilent Technologies).

### Data analysis for gene chip

The specific analysis procedure has been reported previously. First, the raw data were normalized and further classified by PCA. Differentially expressed genes (DEGs) were then selected with a fold change > 2.0 and a $p$-value < 0.05.

### Reagents and antibodies

The mouse polyclonal antibody anti-IFIT1 (ab70023), rabbit monoclonal antibody ALOX15 (ab244205), mouse monoclonal NeuN antibody (ab104224) and rabbit monoclonal GAPDH antibody (ERP16891) were all purchased from Abcam company.

### Primary cortical neuronal cultures and HEK 293T cells

Primary culture of cortical neurons was previously reported [24]. Excitotoxicity was induced by the treatment of neurons with kainic acid (KA) at 1 nmol/l, the same as that used in previous analyses [24]. For pharmaceutical intervention, cells were treated with si-RP11, miR-6756-5p antagonist, or miR-6756-5p mimic. HEK 293T cells were cultured in Dulbecco's modified Eagle medium with D-glucose and 10% fetal bovine serum (FBS). For RP11 overexpression, $3 \times 10^6$ HEK 293T cells were transfected with the RP11-HA plasmid constructed by amplifying the genomic cDNA according to the manufacturer's recommendation (pcDNA3.1/N-HA vector, Clontech, Oxon, UK).

### Mouse TBI model, qRT-PCR, western blot, and immunofluorescence

Lateral fluid percussion injury (FPI) surgery was performed in 6- to 8-week-old male C57-B6 mice, as described previously [11]. The qRT-PCR primer sequences are listed in Supplementary Table SII. Relative expression was calculated with the formula: $2^{-\Delta\Delta Ct}$, $\Delta\Delta Ct = (Ct_{\text{target gene}} - Ct_{\beta\text{-actin}})$ TBI – $(Ct_{\text{target gene}} - Ct_{\beta\text{-actin}})$ control. Experiments were repeated at least three times. The immunofluorescence (IFC) method was previously reported as well [15]. In this study, we probed the brain tissues with NeuN and Alox15 overnight and the secondary antibody was HRP.

### Neurobehavioral assessment

The modified neurological severity score (mNSS) test was used to evaluate neurological function. The test was performed before TBI and on days 1, 3, 7 and 14 after TBI. The scale ranges from 0 to 18 points (normal score, 0 points; maximum deficit score, 18). The mNSS consists of movement (muscle state and abnormal movement), sensation (vision, touch and proprioception), reflex response and balance tests. If the mouse fails to complete the test or does not respond as expected, 1 point is scored; therefore, the higher the score, the more severe the injury [9].

### Nuclear fractionation

$1 \times 10^7$ neurons were collected and washed with RNase-free PBS. After incubation with fraction buffer (Thermo Fisher, 78833) for 15 min on ice, cells were centrifugated at 2500 rpm for another 15 min, and the pellet containing nuclear fractions was selected for RNA extraction.

### FISH assay

The sub-localization of RP11-704M14.1 in neurons was identified using FISH according to the instructions of RiboTM RP11-704M14.1 FISH Probe Mix (Green; Guangzhou Ribo Biology Co., Ltd., Guangzhou, Guangdong, China). The neurons were seeded into the plate at $6 \times 10^4$ cells/well and cultured until the cell confluency reached about 80%. Then, the neurons were fixed by 1 ml of 4% paraformaldehyde, treated with proteinase K (2 µg/ml; Sigma-Aldrich Chemical Company, St Louis, MO, USA), glycine (YZ-140689; Beijing solarbio science and technology Co., Ltd., Beijing, China) and acetamidine reagent. The slides were then incubated with 250 µl of pre-hybridization solution at 42°C for 1 h and with 250 µl of 300 ng/ml hybridization solution containing RP11 probe overnight at 42°C. After that, the slides were stained for 5 min with DAPI (ab104139, 1 : 100, Abcam Inc., Cambridge, UK) diluted using PBS-Tween 20. The slides were then mounted with an anti-fluorescent quencher. Three different fields were selected under a fluorescence microscope (Olympus Optical Co., Ltd, Tokyo, Japan) for observation and photographs.

### Overexpression and knockdown assays

Plasmid-mediated RP11-704M14.1 overexpression and knockdown vector were obtained from WCgene (Shanghai, China), while siRNAs targeting RP11 were obtained from GenePharma (Suzhou, China). The miR-6756-5p mimic was obtained from RiboBio (Guangzhou, China), and the lentiviral expression vectors with the miR-6756-

5p inhibitor and control plasmid were obtained from GeneCopoeia (Rockville, MD, USA). For stable transfections, puromycin was used to select cells stably expressing RP11-704M14.1 and negative vector. The plasmid vectors were incubated with cells for *in-vitro* studies and injected into the ipsilateral ventricles of TBI mice for *in-vivo* studies.

### CCK-8 assay

Each group of cells was adjusted to 1,000 cells per well. 10 µl of CCK-8 solution (Beyotime Biotechnology, Shanghai, China) was added to the cell dish. Only the CCK-8 solution was added to a well as the blank control. Absorbance (OD) in each well was read at 450 nm and tested every 24 h for 3 days.

### RIP assay

The RIP assay was performed using the EZ-Magna RiP Kit (Millipore, Billerica, MA, USA). Cells were lysed in lysis buffer and further incubated with magnetic beads together with human anti-Ago2 (Millipore) or normal human IgG control (Millipore). The immunoprecipitation (IP) RNAs were extracted with Trizol and assessed by qRT-PCR.

### Luciferase reporter assay

A luciferase assay was carried out as previously reported [25]. Primary cultured neurons ($5 \times 10^4$ cells per well) were selected in a 96-well plate and incubated for one day. The plasmids were transfected using Lipofectamine 3000 (Thermo Fisher Scientific, Waltham, MA, USA). After 2 days of transfection, luciferase signals were assessed using a luciferase assay (E1980; Promega, Madison, WI, USA). The binding site for *Alox15* and miR-6756-5p was predicted using: TargetScan [26], miRDB [27] and miRCarta [28]. In addition, RP11 sequences containing the putative wild-type or mutant binding sites for several miRNAs were separately cloned into pmirGLO vector (Promega, Madison, WI, USA). The pmirGLO-RP11-WT reporter and pmirGLO- RP11-Mut reporter were co-transfected into cells with miRNA mimics, miR-NC and other miRNA mimics with Lipofectamine 3000. On day 3, the luciferase reporter assay was carried out.

### Statistical analysis

All data are presented as the mean ± standard error mean (SEM). GraphPad Prism 8.3.1 (San Diego, CA, USA) was used for statistical analyses. Differences among more than two groups were analyzed using one-way ANOVA and subsequently the LSD test or Student's *t*-test, as they were normally distributed. Repeated one-way ANOVA was used to analyze results of CCK-8 and behavioral assays. Spearman correlation analysis was used to assess the relationship between two parameters, such as *ALOX15* and *IFIT1* with GCS. $P < 0.05$ was considered significant.

## Results

### The relationship between *Ifit1* and ENST00000505646.1 in TBI

All cells obtained from GSE 160763 (sc-RNA seq data) were grouped into 11 clusters using the t-SNE map. The 11 clusters were further annotated with SingleR (Figure 1 A). We found that most cells were annotated as astrocytes, neurons, endothelial cells, epithelial, macrophages, microglia, NK cells and T cells. To classify the major cell types in the brain after TBI, we determined the necroptosis score (NCPTS) to classify the cluster using Seurat and identified high NCPTS in endothelial cells, neurons, astrocytes and microglia (Figure 1 B). We found that Ifit1 was dominantly distributed in endothelial cells (Figure 1 C) and related to high NCPTS (Figure 1 D), and this indicated that Ifit1 might be involved in the necroptosis following TBI, which was further verified using chipset data, as previously reported [18] (Supplementary Figure S1). We then evaluated the expression of the marker gene *Ifit1* in different clusters (Figure 1 D). Next, we looked at the cell-cell interaction between control (Figures 1 E–H) and TBI (Figures 1 I–L) groups, and we found both outgoing and incoming signaling patterns reduced in TBI compared to the control group. It is interesting to note that the interaction between astrocytes and neurons and oligodendrocytes decreased in TBI, which suggests that the supporting role of astrocytes decreased following brain injury.

We further analyzed the expression of *IFIT1* in the TBI chipset dataset. *IFIT1* expression was decreased in patients with TBI and was significantly associated with the severity of brain injury (Figures 2 A, B, severe and moderate TBI groups compared to the control group, $p < 0.05$). Detailed information for TBI patients is listed in Supplementary Table SI. *Ifit1* was experimentally found to bind to RNA; accordingly, we conducted co-expression analysis of lncRNAs co-expressed with *Ifit1* and brain injury-related lncRNAs. Only the lncRNA ENST00000505646.1, named RP11-704M14.1, was identified in the intersection (Figure 2 C). We have previously reported that ENST00000505646.1 expression was significantly decreased in patients with severe TBI [18]. However, its role has not been explored in brain injury. We found that the expression of RP11-704M14.1 was positively correlated with expression of *IFIT1* (Figure 2 D), which were both decreased in patients with TBI, and the expression levels were

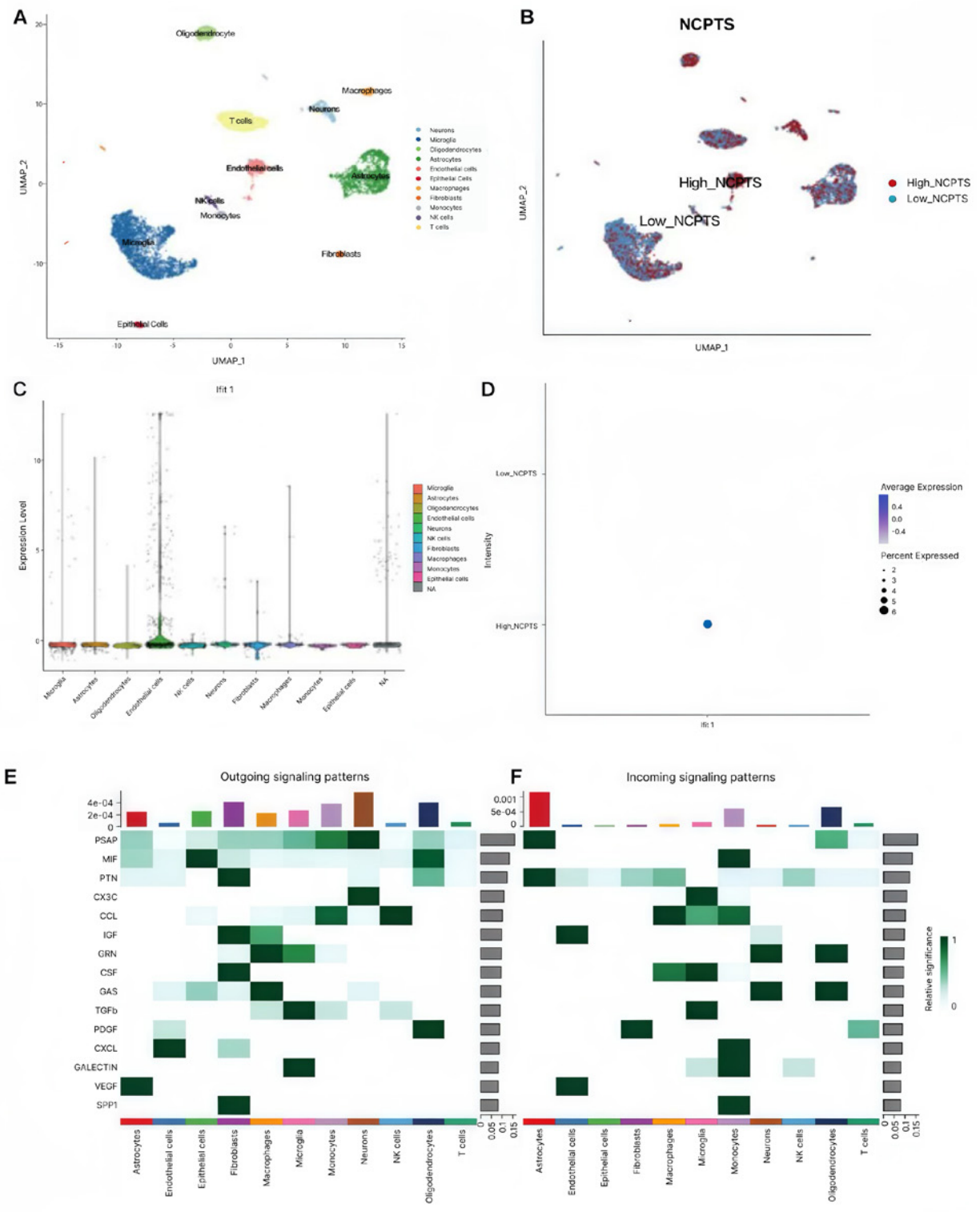


**Figure 1.** Single cell RNA sequencing data in TBI. **A** – Cell cluster annotation in TBI with UMAP. **B** – High and low NCPTS in different clusters. **C** – Ifit1 expression in different cell clusters. **D** – Ifit1 is mainly in the high NCPTS group. **E**–**F** – Cell-cell interaction in control group

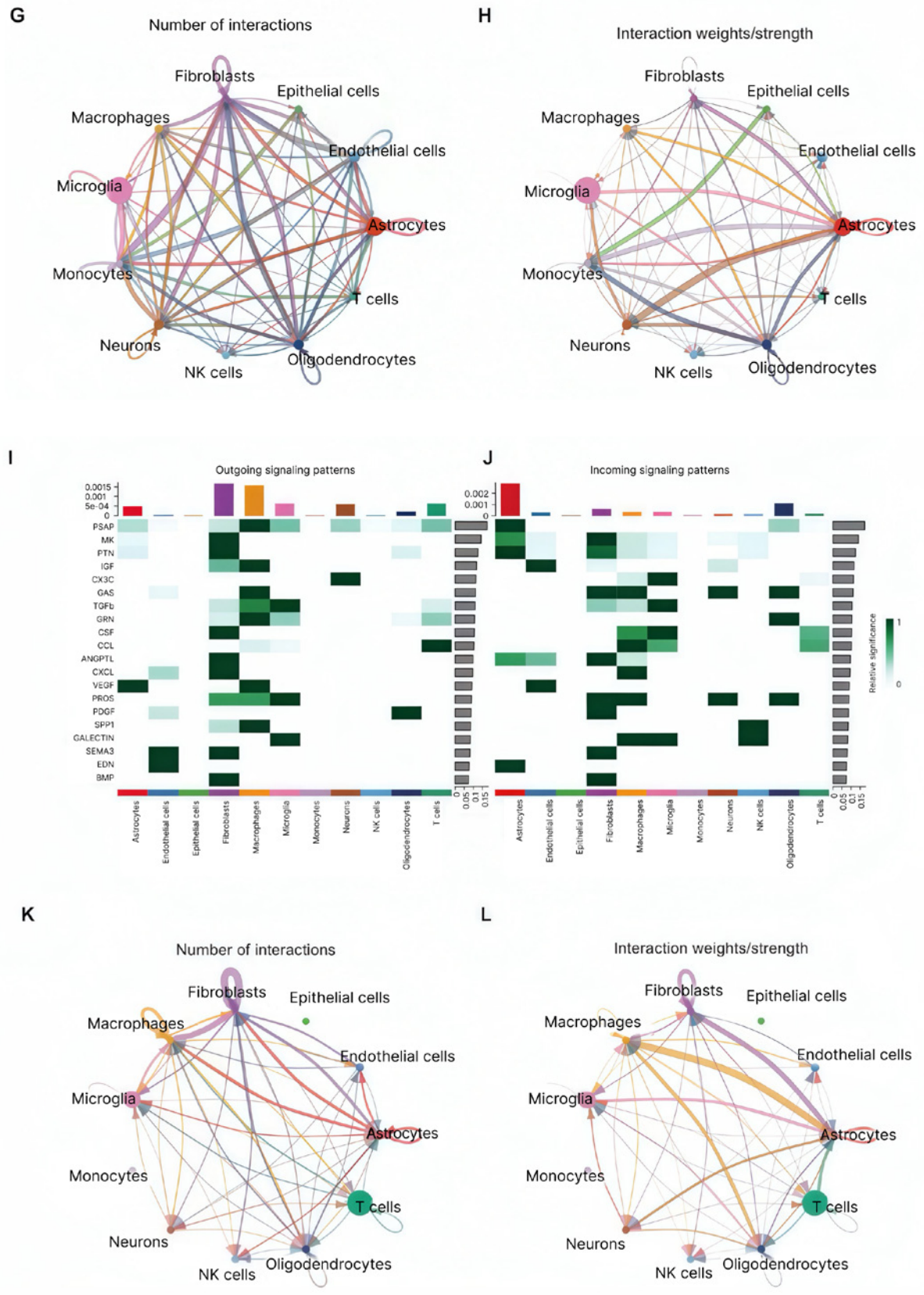


**Figure 1.** Cont. **G–H** – Cell-cell interaction in control group. **I–L** – Cell-cell interaction in TBI group

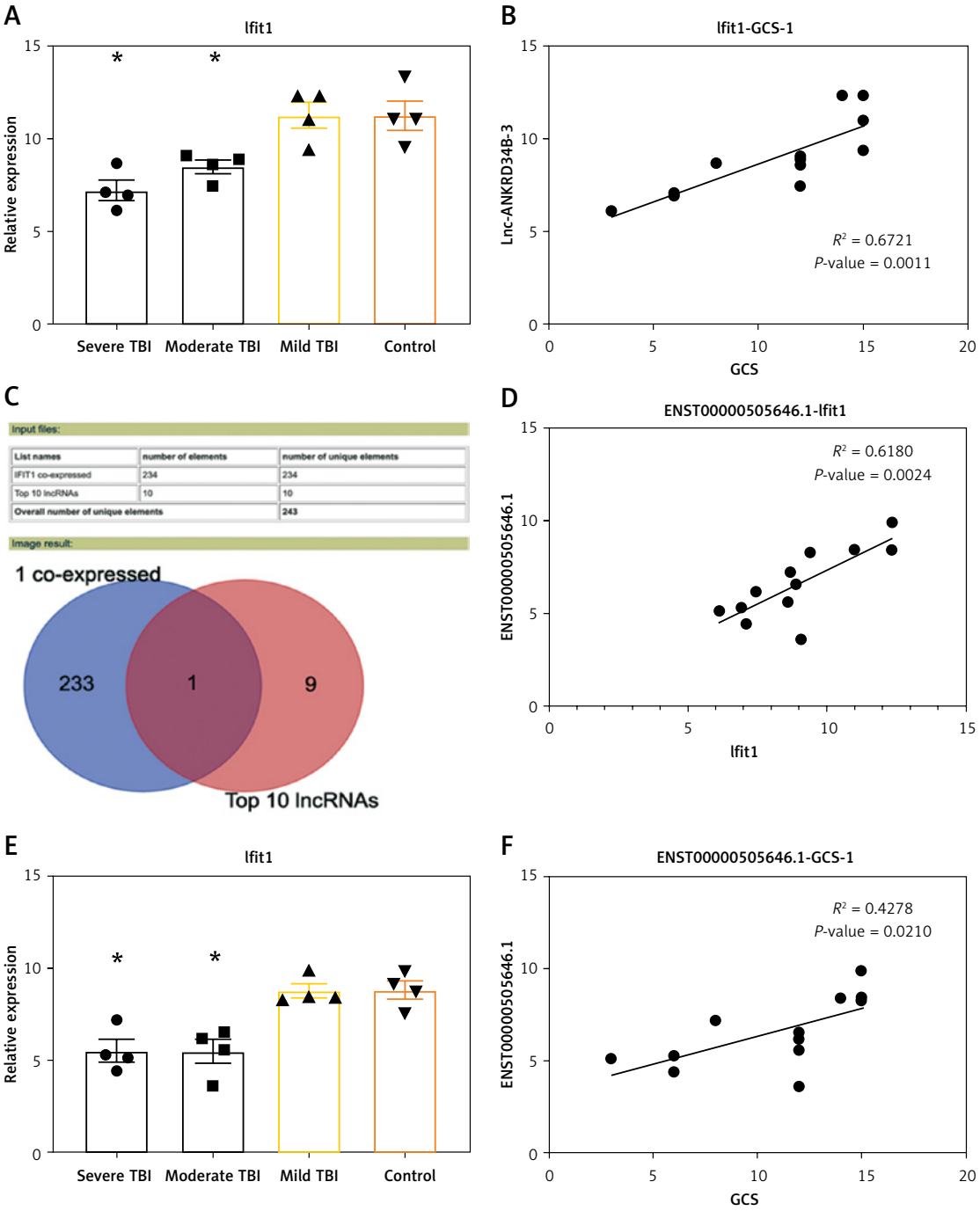


**Figure 2.** Relationship between *IFIT1* and ENST00000505646.1 in TBI. **A**, **B** – Plasma *IFIT1* decreased with the severity of brain severity with a significant correlation. **C**, **D** – Co-expression of *IFIT1* and ENST00000505646.1. **E**, **F** – ENST00000505646.1 expression decreased significantly with the severity of brain injury. *a significant difference compared to the control group, $p < 0.05$. The number of replicates is 4 in each group and the error bar is mean ± SEM (standard error of mean)

significantly associated with the severity of brain injury (Figures 2 E, F).

## RP11-704M14.1 silencing inhibits neuronal proliferation

To elucidate the neurological role of RP11-704M14.1, primary cultured neurons with siRNA, a lentiviral recombinant siRNA vector (vector), or a lentiviral recombinant overexpression plasmid was used to knock down or overexpress RP11-704M14.1 (Figures 3 A, B). A CCK-8 assay showed that RP11-704M14.1 knockdown significantly inhibited the proliferation of neurons, while RP11-704M14.1 overexpression promoted neuronal growth (Figures 3 C, D).

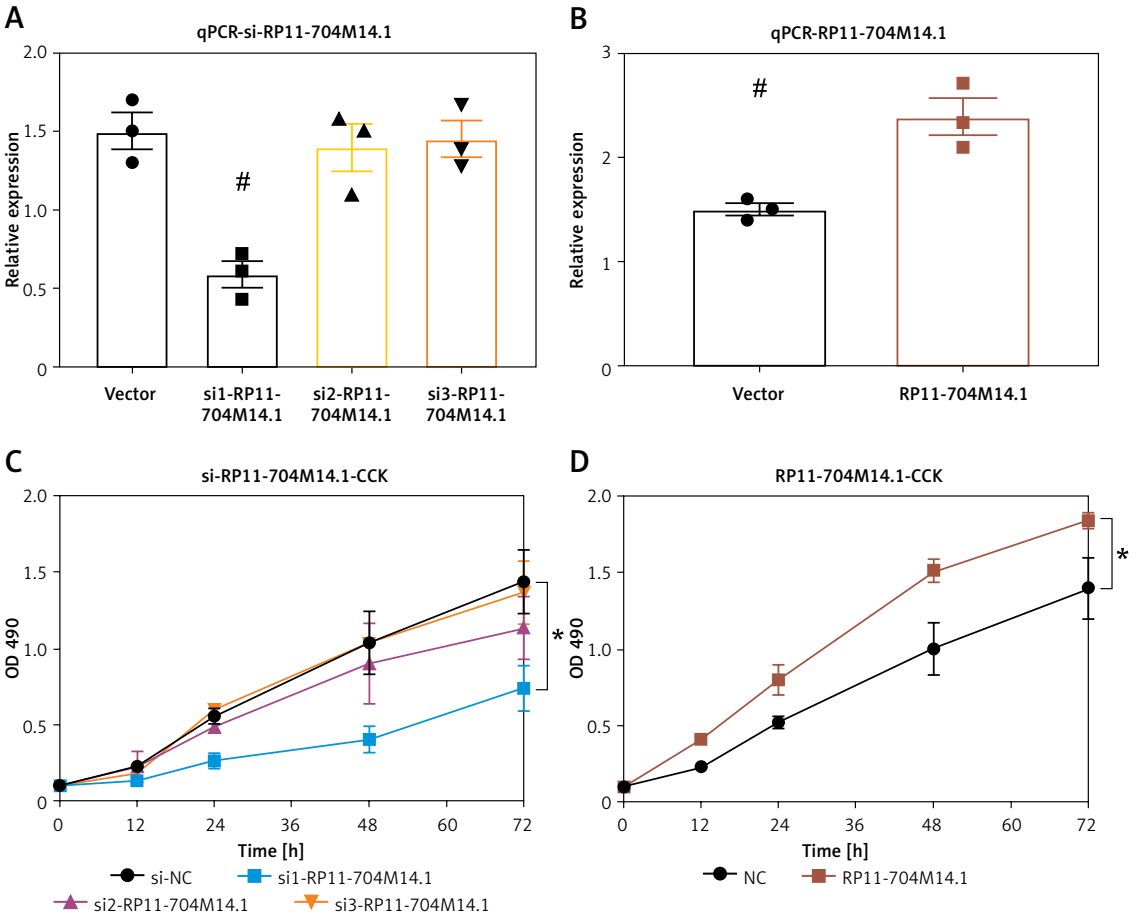


**Figure 3.** Effects of lncRNA RP11-704M14.1 on neuronal proliferation. **A**, **B** – Verification of RP11-704M14.1 knockdown and overexpression. **C** – After primary cortical neurons were transfected with siNC or si-RP11-704M14.1, a CCK-8 assay was performed to assess cell proliferation. **D** – Primary cortical neurons were transfected with NC or RP11-704M14.1, and cell proliferation was assessed using a CCK-8 assay. $^{\#}p < 0.05$ (compared to the vector group); $^{*}p < 0.05$ (compared to the control group: siNC or NC). The scale bar is 100 µm. The number of replicates is 3 in each group and the error bar is mean ± SEM

## RP11-704M14.1 promotes neuronal and ALOX15 expression in TBI mice

To validate the *in-vitro* effect of RP11-704M14.1 on the proliferation in primary cultured neurons, we injected the plasmid-mediated RP11-704M14.1 into the ipsilateral ventricle of TBI mice just after the brain injury was modeled. We found that overexpression of RP11-704M14.1 could increase the neuronal level and ALOX15 expression reflected by their positive counting at 24 h after injury (Supplementary Figure S2). Meanwhile, RP11-704M14.1 was able to decrease the mNSS in TBI mice as well (Supplementary Figure S2), which indicates that RP11-704M14.1 has a neuroprotective effect in TBI.

## RP11-704M14.1 acts as a molecular sponge for miR-6756-5p in neurons

To explore the role of RP11-704M14.1 in neurons, we first analyzed its subcellular location using fluorescence in situ hybridization (FISH). We found that the expression of RP11-704M14.1 was predominant in the cytosol (Figure 4 A), indicating that it might function at the post-transcriptional level. We used a bioinformatical approach to predict miRNAs that bind to the RP11-704M14.1, using miRbase. We detected potential binding between RP11-704M14.1 and hsa-miR-6756-5p (Figure 4 B). RNA immunoprecipitation (RIP) using an Ago2 antibody revealed that RP11-704M14.1 binds directly to Ago2 in neurons, indicating that this lncRNA might be involved in miRNA binding (Figure 4 C). Next, we analyzed our ceRNA chipset data from plasma of patients with TBI and found that hsa-miR-6756-5p is a potential binding miRNA for RP11-704M14.1. We evaluated the activity of RP11-704M14.1 using a luciferase reporter assay after site-directed mutagenesis of the putative miR-6756-5p binding site. As expected, the luciferase reporter assay showed that miR-6756-5p directly targets the 3'UTR of lncRNA RP11-704M14.1-WT to negatively regulate the luciferase activity of lncRNA RP11-704M14.1-wt-3'UTR but not lncRNA RP11-704M14.1-MUT's 3'UTR (Fig-

A

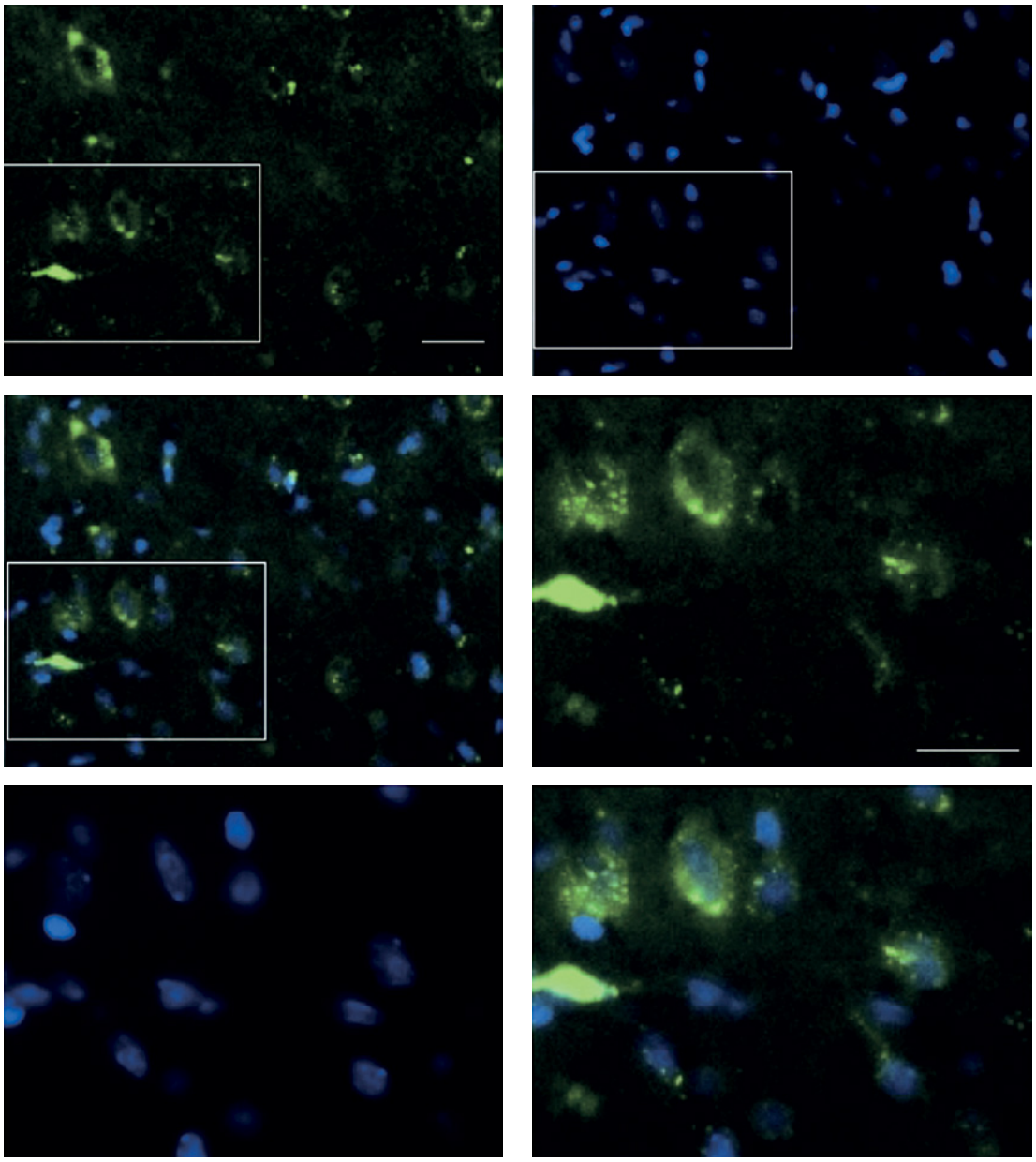

B

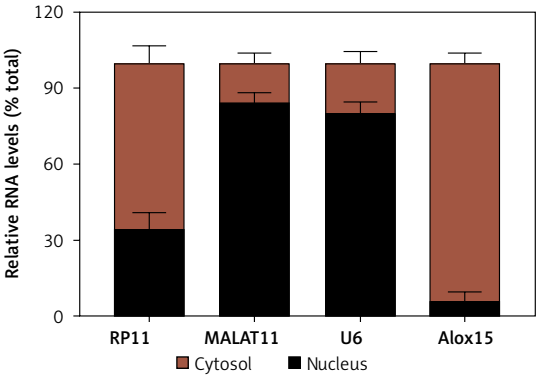


C

| Gene | miRNA | Score | DIANA Links |
|---|---|---|---|
| RP11-704M14.1 | hsa-miR-548bb-5p | 0.495 | mT TB InE mP |
| RP11-704M14.1 | hsa-miR-548au-5p | 0.495 | mT TB InE mP |
| RP11-704M14.1 | hsa-miR-6820-3p | 0.494 | mT TB InE mP |
| RP11-704M14.1 | hsa-miR-7843-3p | 0.494 | mT TB InE mP |
| RP11-704M14.1 | hsa-miR-200b-5p | 0.493 | mT TB InE mP |
| RP11-704M14.1 | hsa-miR-580-3p | 0.493 | mT TB InE mP |
| RP11-704M14.1 | hsa-miR-3193 | 0.493 | mT TB InE mP |
| RP11-704M14.1 | hsa-miR-6756-5p | 0.493 | mT TB InE mP |

**Figure 4.** RP11-704M14.1 binds with miR-6756-5p in neurons. **A** – FISH assay showed that RP11-704M14.1 was predominantly located in cytoplasm of neurons, and the enlarged figures are also shown. **B** – Subcellular fractionation assays showed the subcellular distribution of RP11-704M14.1 and Alox15 in neurons. U6 and MALAT1 were used as a nuclear control. **C** – Based on an interactome prediction, six miRNAs were predicted to bind to RP11-704M14.1

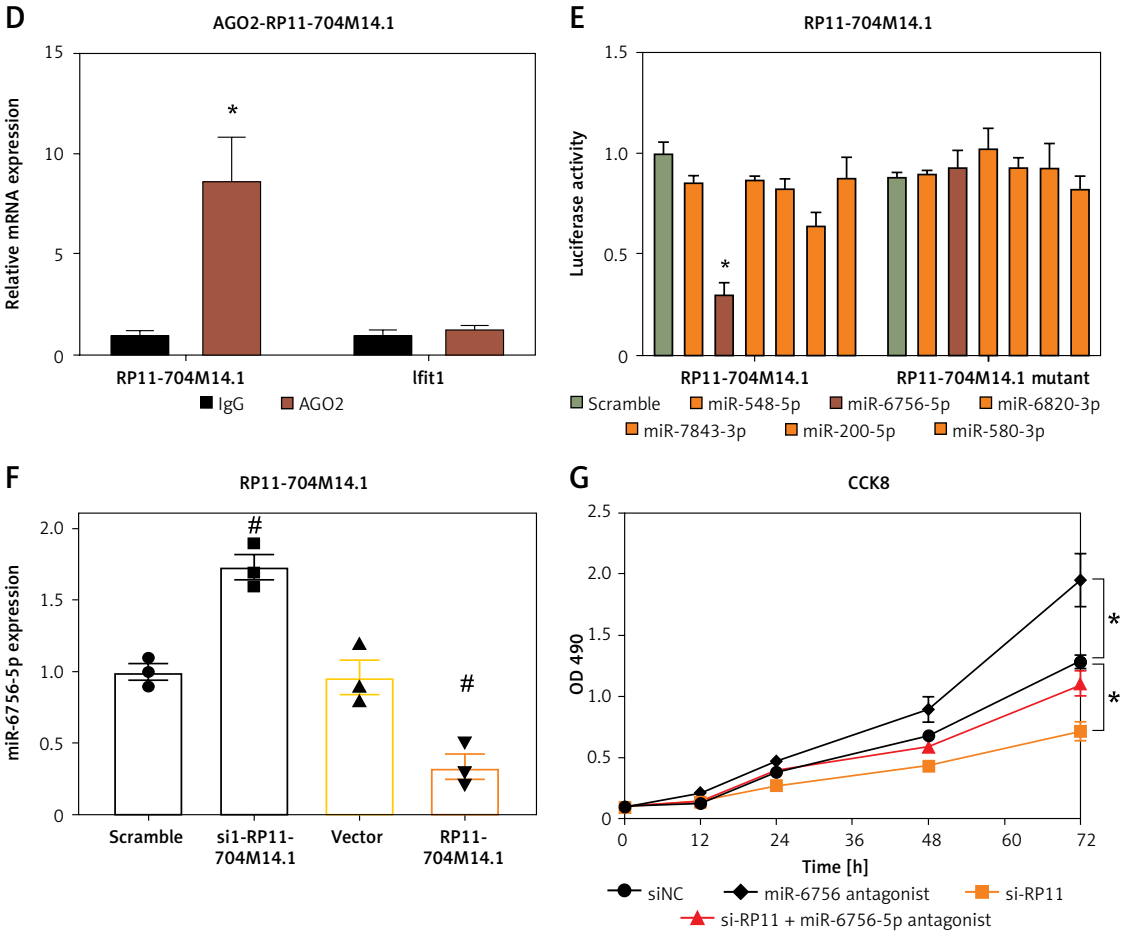


**Figure 4.** Cont. **D** – RP11-704M14.1 was predicted to have an association with AGO2 (a miRNA-binding protein), and RIP assay showed that AGO2 binds to RP11-704M14.1, *$p < 0.05$, relative mRNA expression compared between IgG and AGO2. **E** – Primary cultured neurons were co-transfected with each miRNA mimic and the RP11-704M14.1 wild-type reporter or RP11-704M14.1 mutant reporter; the *y*-axis shows the luciferase intensity. A scrambled mimic was used as a control, *$p < 0.05$, luciferase activity compared between miRs and scramble. **F** – After primary cultured neurons were transfected with si-NC (scramble), si- RP11-704M14.1, vector and RP11-704M14.1, the expression level of miR-6756-5p was assessed, #$p < 0.05$, compared to scramble or vector, respectively. **G** – After primary cultured neurons were transfected with siNC, si-RP11-704M14.1, miR-6756-5p antagonist, and si-RP11-704M14.1+ miR-6756-5p antagonist, cell viability was assessed using a CCK-8 assay; *$p < 0.05$. The number of replicates is 3 in each group and the error bar is mean ± SEM. Bar = 20 µm

ure 4 D). Furthermore, we found that the knockdown of lncRNA RP11-704M14.1 significantly increased the expression level of miR-6756-5p in neurons (Figure 4 E). Overexpression of RP11-704M14.1 significantly inhibited the expression of miR-6756-5p (Figure 4 E). In addition, a CCK-8 assay showed that si-RP11-704M14.1 could reduce cell proliferation, and this effect was rescued by a miR-6756-5p antagonist. Interestingly, the miR-6756-5p antagonist increased the neuronal proliferation. These results prompted us to investigate predicted targets of miR-6756-5p (Figure 4 F).

## *ALOX15* is a miR-6756-5p target gene and is indirectly regulated by lncRNA RP11-704M14.1

To determine the ceRNA regulatory network linking lncRNA RP11-704M14.1, miR-6756-5p, and downstream targets, we used various algorithms (TargetScan, miRDB, and miRCarta) to predict potential miR-6756-5p targets. Additionally, we verified the lncRNA RP11-704M14.1-miR-6756-5p ceRNA network based on expression levels in our TBI chipset dataset and found that 49 intersected genes may be involved in this network (Supplementary Figure S3). In addition, only *ALOX15* was found in the intersection of the 49 target genes with the top 10 altered mRNAs in patients with TBI (Supplementary Figure S4). Arachidonate 15-lipoxygenase, encoded by ALOX15, is involved in the regulation of apoptosis. We performed a luciferase reporter gene assay driven by the wild-type 3'UTR sequence of *ALOX15* containing the predicted miR-6756-5p-binding site (wt-*ALOX15*), or mutant constructs containing a mutation in the miR-6756-5p-binding site (mut-*ALOX15*).

These plasmids were co-transfected into human embryonic kidney (HEK) 293T cells with non-targeting control miRNA, miR-6756-5p mimics and miR-6756-5p inhibitor. Co-transfection with the miR-6756-5p mimic resulted in significantly lower wt-*ALOX15*-driven luciferase expression than that in the control. Co-transfection with the miR-6756-5p inhibitor increased wt-*ALOX15*-driven luciferase expression, but this change was not detected for the mutant miR-6756-5p binding site (Figure 5 A).

To determine the effect of the RP11-704M14.1-miR-6756-5p axis in vivo, we measured the protein levels of IFIT1 and ALOX15 in the ipsilateral cortex of a mouse model of TBI when the RP11-704M14.1-miR-6756-5p axis was manipulated. We found that TBI reduced the IFIT1 and ALOX15

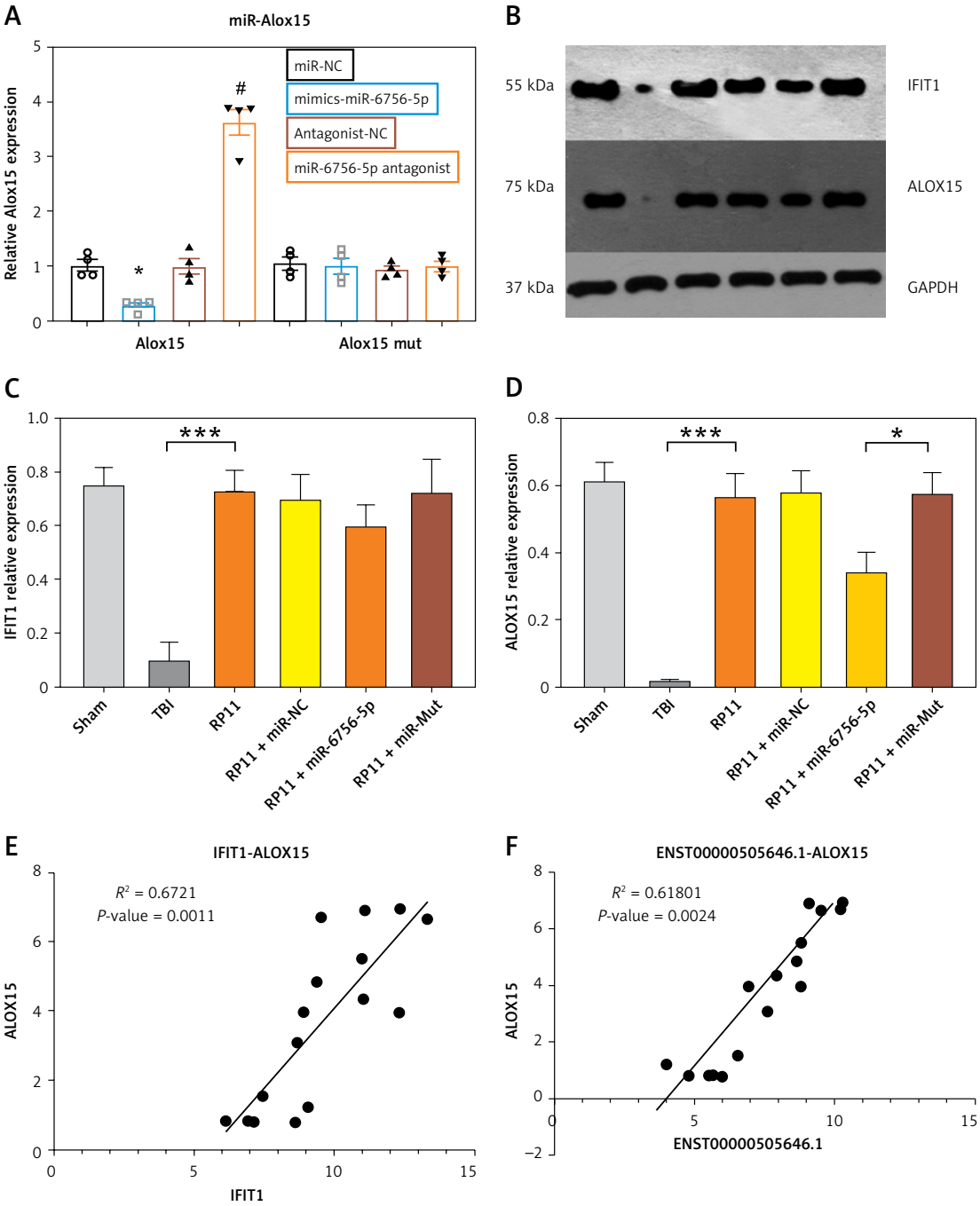


**Figure 5.** *Alox15* is a miR-6756-5p target gene and is indirectly regulated by lncRNA RP11-704M14.1. **A** – After primary cultured neurons were transfected with NC, miR-6756-5p, antagonist NC and miR-6756-5p antagonist, the mRNA level of *Alox15* was assessed; $^{*,\#}p < 0.05$, compared to NC group. **B** – IFIT1 and ALOX15 levels in TBI depending on RP11-704M14.1 and miR-6756-5p. **C**, **D** – Quantification of western blotting results in Figure B. **E**, **F** – Correlations between levels of IFIT1, ALOX15, and ENST00000505656.1. The number of replicates is 4 in each group and the error bar is mean ± SEM

levels. RP11-704M14.1 treatment in TBI models increased the expression of both IFIT1 and ALOX15 (Figure 5 B). The increase in ALOX15 levels was rescued by miR-6756-5p but not by the miR-NC and mutant miR-6756-5p. In addition, the IFIT1 level was only affected by RP11-704M14.1, but not miR-6756-5p or its negative control and mutant form (Figures 5 C, D). Since RP11-704M14.1 influenced the expression of both IFIT1 and ALOX15, we investigated their relationship using our ceRNA chipset data and found that the expression of ALOX15 was positively associated with IFIT1 and RP11-704M14.1 levels (Figures 5 E, F). A cluster analysis of the top 10 lncRNAs and 10 mRNAs showed that both *IFIT1* and RP11-704M14.1 can differentiate between moderate and severe groups and mild plus control groups (Supplementary Figure S3). Taken together, these data suggest that the regulation of *Alox15* expression regulation is primarily mediated by post-transcriptional regulation of miR-6756-5p via lncRNA RP11-704M14.1.

## Discussion

Recent investigations have highlighted the significance of long noncoding RNAs (lncRNAs) in central nervous system (CNS) disorders, including traumatic brain injury (TBI) [6, 7, 14, 25]. Despite these advances, the specific functions of lncRNAs in TBI remain to be fully elucidated. Our study integrates single-cell RNA sequencing (scRNA-seq) with ceRNA chipset data, revealing that Ifit1 downregulation is associated with TBI. We identified Ifit1 as a marker gene through clustering analysis. Subsequent co-expression analysis, combined with in vitro and in vivo assays, confirmed the involvement of the ceRNA axis RP11-704M14.1–miR-6756-5p–ALOX15 in TBI.

Interestingly, RP11-704M14.1 has been shown to be significantly upregulated in post-menopausal osteoporosis, contributing to apoptotic processes and enhancing NF-κB signaling [29]. Of note, *ALOX15* is traditionally considered to have a pro-inflammatory effect and may play a key role in the acute inflammatory response [30]. *Alox15* gene expression was increased in an animal model of colitis, and systemic *Alox15* deficiency induces less inflammation [31]. In contrast, the transgenic overexpression of human *ALOX15* exacerbates inflammatory symptoms in animal models [32]. The short-term administration of atorvastatin in a model of cerebral ischemia has been shown to downregulate *Alox15* expression and reduce brain damage [33]. However, recent studies show that *Alox15* inhibition or antisense oligonucleotide-mediated knockdown in the prefrontal cortex also blocks the long-term potentiation of the hippocampus-prefrontal cortex pathway and increases errors in alternation in the T-maze test via reducing D1 receptor activation [34]. *In vivo* studies have also shown that the knockout of *Alox15* impairs adipocyte proliferation/differentiation [35]. The loss of *Alox15* reduced PI-3K/Akt and β-catenin signaling and decreased the rate of cell proliferation [36]. In line with our findings, Alox15 expression was found to decrease in a rat TBI model, with progesterone treatment enhancing Alox15 mRNA levels, suggesting a neuroprotective effect [37]. Erythropoietin treatment after TBI also upregulates Alox15 expression. We explored the RP11-704M14.1-miR-6756-5p-ALOX15 axis's impact on cellular proliferation *in vivo*. Our data indicate that RP11-704M14.1 knockdown significantly curtails cellular proliferation, an effect partially reversed by a miR-6756-5p antagonist. The discrepancies between previous findings and ours regarding Alox15's role may stem from differing neurological disease contexts and the diverse immune and inflammatory cell profiles within neuronal microenvironments [38]. Therefore, comprehensive assessments of Alox15's contribution to TBI, including Alox15 siRNA or knockout mice studies, are warranted.

Several limitations need to be addressed. We have previously found that the number of altered lncRNAs and mRNAs increases with the severity of TBI. The precise changes in the expression level and functions of lncRNAs after brain insults are still unclear and could involve DNA-, RNA-, and protein-level modifications [18]. Interferon-induced protein with tetratricopeptide repeats 1, encoded by *IFIT1*, belongs to the interferon-induced antiviral RNA-binding protein family; it is primarily located in the cytoplasm and can bind specifically to single-stranded RNA bearing a 5′-triphosphate group (PPP-RNA) and inhibit the expression of viral mRNAs [39]. Single-stranded PPP-RNAs, which lack the 2′*O*-methylation of the 5′ cap, are considered to be foreign nucleic acids from viruses, fungi, bacteria, or other parasites [40]. The 5′ cap is critical for host interferon-induced proteins to distinguish between self and non-self mRNAs as a molecular signature with a cap snatching mechanism [41]. Therefore, it is essential to investigate the relationship between Ifit1 and lncRNAs in the future to verify this new modification. Meanwhile, *Ifit1* is a marker gene mainly located in cluster 9, and both cluster 9 (endothelial) and 20 (epithelial) are mostly enriched clusters in our studies. This indicates that Ifit1 and the related RP11-704M14.1-miR-6756-5p-*Alox15* axis might have a critical role in the blood-brain barrier in TBI, which is of interest for future study as well.

In conclusion, our results show that RP11-704M14.1 promotes neuronal proliferation by sponging miR-6756-5p and regulating *ALOX15*

expression in brain insults; accordingly, targeting this lncRNA presents a promising avenue for TBI.

## Acknowledgments

Cao Ke, Gong Ru, Wang Jiancun contribute equally to the work.

## Funding

This study was funded by the Key Medical Discipline Group Construction Project of Shanghai Pudong New area (PWZxq2022-13).

## Ethical approval

The study protocol was approved by the local Ethics Committee in Shanghai Pudong New area People's Hospital (20170223-001 on March 7, 2017). The informed consent form was obtained as required.

All authors approved the final version and agreed with the submission.

## Conflict of interest

The authors declare no conflict of interest.

## References

1. GBD 2016 Traumatic Brain Injury and Spinal Cord Injury Collaborators. Global, regional, and national burden of traumatic brain injury and spinal cord injury, 1990-2016: a systematic analysis for the Global Burden of Disease Study 2016. Lancet Neurology 2019; 18: 56-87.
2. Yin X, Shen L, Zhou L, et al. Duodenal versus gastric feeding in patients with traumatic brain injury: a systematic review and meta-analysis. Arch Med Sci 2022; https://doi.org/10.5114/aoms/147593.
3. Lu S, Yang X, Wang C, et al. Current status and potential role of circular RNAs in neurological disorders. J Neurochem 2019; 150: 237-48.
4. Zhang L, Wang H. Long non-coding RNA in CNS injuries: a new target for therapeutic intervention. Mol Ther Nucleic Acids 2019; 17: 754-66.
5. Shan W, Chen W, Zhao X, et al. Long noncoding RNA TUG1 contributes to cerebral ischaemia/reperfusion injury by sponging mir-145 to up-regulate AQP4 expression. J Cell Mol Med 2020; 24: 250-9.
6. Zhang X, Liu Z, Shu Q, et al. LncRNA SNHG6 functions as a ceRNA to regulate neuronal cell apoptosis by modulating miR-181c-5p/BIM signalling in ischaemic stroke. J Cell Mol Med 2019; 23: 6120-30.
7. Wang CF, Zhao CC, Weng WJ, et al. Alteration in long non-coding RNA expression after traumatic brain injury in rats. J Neurotrauma 2017; 34: 2100-8.
8. Li Z, Han K, Zhang D, et al. The role of long noncoding RNA in traumatic brain injury. Neuropsychiatr Dis Treat 2019; 15: 1671-7.
9. Patel NA, Moss LD, Lee JY, et al. Long noncoding RNA MALAT1 in exosomes drives regenerative function and modulates inflammation-linked networks following traumatic brain injury. J Neuroinflamm 2018; 15: 204-23.
10. Yang L, Xu Y, Zhang W. Sophoricoside attenuates neuronal injury and altered cognitive function by regulating the LTR-4/NF-κB/PI3K signalling pathway in anaesthetic-exposed neonatal rats. Arch Med Sci 2020; 20: 248-54.
11. Jiang YJ, Cao SQ, Gao LB, et al. Circular ribonucleic acid expression profile in mouse cortex after traumatic brain injury. J Neurotrauma 2019; 36: 1018-28.
12. Huang S, Ge X, Yu J, et al. Increased miR-124-3p in microglial exosomes following traumatic brain injury inhibits neuronal inflammation and contributes to neurite outgrowth via their transfer into neurons. FASEB J 2018; 32: 512-28.
13. Wu J, He J, Tian X, et al. microRNA-9-5p alleviates blood-brain barrier damage and neuroinflammation after traumatic brain injury. J Neurochem 2020; 153: 710-26.
14. Ding Y, Zhu W, Kong W, et al. Edaravone attenuates neuronal apoptosis in hippocampus of rat traumatic brain injury model via activation of BDNF/TrkB signaling pathway. Arch Med Sci 2021; 17: 514-22.
15. He B, Chen W, Zeng J, et al. Long noncoding RNA NKILA transferred by astrocyte-derived extracellular vesicles protects against neuronal injury by upregulating NLRX1 through binding to mir-195 in traumatic brain injury. Aging 2021; 13: 8127-45.
16. Tao Z, Guo H, Tang J, Cheng M. Knockdown of SNW1 ameliorates brain microvascular endothelial cells injury by inhibiting NLRP3 inflammasome activation. Arch Med Sci 2021; https://doi.org/10.5114/aoms/143514.
17. Zheng P, Shu L, Ren D, et al. circHtra1/miR-3960/GRB10 axis promotes neuronal loss and immune deficiency in traumatic brain injury. Oxid Med Cell Longev 2022; 2022: 3522492.
18. Ren D, Chen W, Cao K, et al. Expression profiles of long non-coding RNA and messenger RNA in human traumatic brain injury. Mol Ther Nucleic Acids 2020; 22: 99-113.
19. Witcher KG, Bray CE, Chunchai T, et al. Traumatic brain injury causes chronic cortical inflammation and neuronal dysfunction mediated by microglia. J Neurosci 2021; 41: 1597-616.
20. Hao Y, Hao S, Andersen-Nissen E, et al. Integrated analysis of multimodal single-cell data. Biorxiv 2020; 2020.10.12.335331.
21. Aran D, Looney AP, Liu L, et al. Reference-based analysis of lung single-cell sequencing reveals a transitional profibrotic macrophage. Nat Immunol 2019; 20: 163-72.
22. Jin S, Guerrero-Juarez CF, Zhang L, et al. Inference and analysis of cell-cell communication using CellChat. Nat Commun 2021; 12: 1088.
23. Cao J, Spielmann M, Qiu X, et al. The single-cell transcriptional landscape of mammalian organogenesis. Nature 2019; 566: 496-502.
24. Chen W, He B, Tong W, et al. Astrocytic insulin-like growth factor-1 protects neurons against excitotoxicity. Front Cell Neurosci 2019; 13: 298.
25. He B, Chen W, Zeng J, et al. MicroRNA-326 decreases tau phosphorylation and neuron apoptosis through inhibition of the JNK signaling pathway by targeting VAV1 in Alzheimer's disease. J Cell Physiol 2020; 235: 480-93.
26. Agarwal V, Bell GW, Nam JW, Bartel DP. Predicting effective microRNA target sites in mammalian mRNAs. Elife 2015; 4: e05005.
27. Chen Y, Wang X. miRDB: an online database for prediction of functional microRNA targets. Nucleic Acids Res 2019; 48: D127-131.
28. Backes C, Fehlmann T, Kern F, et al. miRCarta: a central repository for collecting miRNA candidates. Nucleic Acids Res 2017; 46: gkx851.

29. Wang S. Investigation of long non-coding RNA expression profiles in patients with post-menopausal osteoporosis by RNA sequencing. Exp Ther Med 2020; 20: 1487-97.
30. Lim CS, Porter DW, Orandle MS, et al. Resolution of pulmonary inflammation induced by carbon nanotubes and fullerenes in mice: role of macrophage polarization. Front Immunol 2020; 11: 1186.
31. Rohwer N, Chiu C, Huang D, et al. Omega-3 fatty acids protect from colitis via an Alox15-derived eicosanoid. FASEB J 2021; 35: e21491.
32. Kroschwald S, Chiu CY, Heydeck D, et al. Female mice carrying a defective Alox15 gene are protected from experimental colitis via sustained maintenance of the intestinal epithelial barrier function. Biochim Biophys Acta Mol Cell Biol Lipids 2018; 1863: 866-80.
33. Zhang P, Xing X, Hu C, et al. 15-Lipoxygenase-1 is involved in the effects of atorvastatin on endothelial dysfunction. Mediat Inflamm 2016; 2016: 6769032.
34. Shalini SM, Ho CFY, Ng YK, et al. Distribution of Alox15 in the rat brain and its role in prefrontal cortical resolvin D1 formation and spatial working memory. Mol Neurobiol 2018; 55: 1537-50.
35. Kwon HJ, Kim SN, Kim YA, Lee YH. The contribution of arachidonate 15-lipoxygenase in tissue macrophages to adipose tissue remodeling. Cell Death Dis 2016; 7: e2285.
36. Chen Y, Peng C, Abraham SA, et al. Arachidonate 15-lipoxygenase is required for chronic myeloid leukemia stem cell survival. J Clin Invest 2014; 124: 3847-62.
37. Anderson GD, Farin FM, Bammler TK, et al. The effect of progesterone dose on gene expression after traumatic brain injury. J Neurotraum 2011; 28: 1827-43.
38. Wang L, Zhao J, Zhu B, et al. Microglia polarization in heat-induced early neural injury. Arch Med Sci 2024; 20: 1307-13.
39. Pichlmair A, Lassnig C, Eberle CA, et al. IFIT1 is an antiviral protein that recognizes 5′-triphosphate RNA. Nat Immunol 2011; 12: 624-30.
40. Choi YJ, Bowman JW, Jung JU. A Talented duo: IFIT1 and IFIT3 patrol viral RNA caps. Immunity 2018; 48: 474-6.
41. Kikkert M. Innate immune evasion by human respiratory RNA viruses. J Innate Immun 2020; 12: 4-20.